Mechanistic insights into the formation of polyion complex aggregates from cationic thermoresponsive diblock copolymers

E. Read, Barbara Lonetti, Stéphane Gineste, A.T. Sutton, E. Di Cola, Patrice Castignolles, Marianne Gaborieau, Anne-Françoise Mingotaud, Mathias Destarac, Jean-Daniel Marty

Graphical abstract. Thermoresponsive polyion complex aggregates were obtained by addition of polyacrylic acid to diblock copolymers based on cationic poly(3-acrylamidopropyltrimethylammonium chloride) and thermoresponsive poly(N-isopropylacrylamide). Temperature induced structural changes on these objects whose reversibility was related to the macromolecular characteristics of the copolymers.

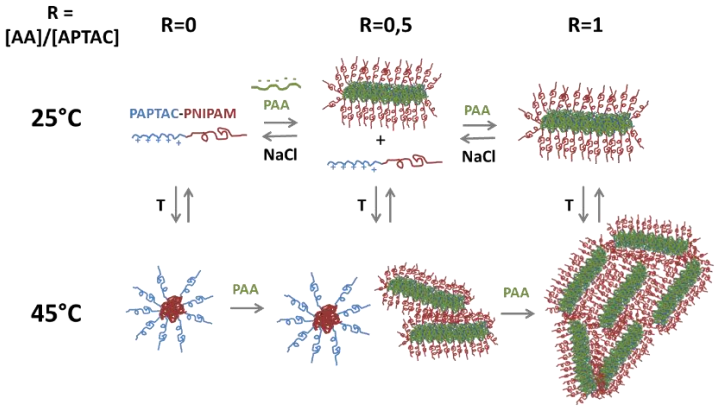

Mechanistic Insights into the Formation of Polyion Complex Aggregates from Cationic Thermoresponsive Diblock Copolymers

E. Read[a], B. Lonetti[a], S. Gineste[a], A. T. Sutton[b,c], E. Di Cola[d], P. Castignolles[b], M. Gaborieau[b], A.-F. Mingotaud[a], M. Destarac[a,*], J.-D. Marty[a,*]

[a] Dr. E. Read, Dr. B. Lonetti, S. Gineste, Dr. A-F. Mingotaud, Prof. Dr. M. Destarac, Ass. Prof. J-D. Marty. Laboratoire des IMRCP, Université Paul Sabatier, CNRS UMR 5623 118 route de Narbonne 31062 Toulouse Cedex 9, France

[b] A. T. Sutton, Dr. P. Castignolles, Dr. M. Gaborieau. Western Sydney University, ACROSS, School of Science, Locked Bag 1797, Penrith NSW 2751, Australia

[c] A. T. Sutton, Future Industries Institute, University of South Australia, P.O. Box 2471, Adelaide, South Australia 5001, Australia

[d] E. Di Cola, SAS-analysis, Saint Egreve, France

*corresponding authors. Tel. +33.56155.6135. E-mail: destarac@chimie.ups-tlse.fr, marty@chimie.ups-tlse.fr

ABSTRACT.

Hypothesis: The formation of polyion complexes (PICs) comprising thermoresponsive polymers is internted to result in the formation of aggregates that undergo significant structural changes with temperature. Moreover the observed modifications might be critically affected by polymer structure and PICs composition.

Experiments: Different block copolymers based on cationic poly(3-acrylamidopropyltrimethylammonium chloride) and thermoresponsive poly(N-isopropylacrylamide) were synthesized by aqueous RAFT/MADIX polymerization at room temperature. Addition of poly(acrylic acid) in a controlled fashion led to the formation of PICs aggregates. The structural changes induced by temperature were characterized by differential scanning calorimetry, Nuclear Magnetic Resonance spectroscopy and scattering methods.

Findings: Thermoresponsive PICs undergo significant structural changes when increasing temperature above the cloud point of the thermoresponsive block. The reversibility of these phenomena depends strongly on the structural parameters of the block copolymers and on PICs composition.

KEYWORDS: double hydrophilic block copolymers, polyion complexes, thermoresponsive polymers, nuclear magnetic resonance spectroscopy, capillary electrophoresis, small-angle X-ray scattering, dynamic light scattering

1. Introduction

Following the extensive work of Kabanov's team in the early nineties, the association between oppositely charged polyelectrolytes has aroused great interest in the past decade.[1] Soluble complexes were obtained when two conditions were fulfilled: (i) the ratio between charged groups differed from unity, (ii) the polyelectrolyte with the higher degree of polymerization was in excess with respect to the other.in terms of number of moles of monomers unit[2] Nevertheless at the equimolar stoichiometry macroscopic precipitation always occurred. The discovery that such a precipitation could be avoided when using block copolymers instead of homopolymers led Kataoka and co-workers to develop the modern version of such assemblies, namely polyion complex micelles (PICs) also called block ionomer complexes, micellar interpolyelectrolyte complexes or complex coacervate core micelles.[3,4] PIC assemblies are generally obtained using at least one double hydrophilic block copolymer (DHBC) with a first neutral block and a second one charged. The other PIC partner consists either in a homo-polyelectrolyte or another double hydrophilic block copolymer with a charged block of opposite charge.

With the development of macromolecular engineering and particularly reversible-deactivation radical polymerization, the number of achievable block copolymers has exploded enabling the easy and controlled formation of polymer-based nanostructured materials. However, the use of DHBCs with a thermoresponsive block that can undergo a morphological transition above a characteristic cloud point temperature (T_c) has scarcely been reported in such assemblies. [5-10] Below T_c the block copolymer is fully soluble in water. The addition of an oppositely charged polymer leads to the formation of self-assembled systems [5,6,7,9,10] and this process generally occurs on a millisecond timescale.[10] Above T_c the thermoresponsive block becomes dehydrated and the copolymer presents an amphiphilic character. This induces spontaneous assembly with a dehydrated core and a charged outer shell. Addition of an oppositely charged polymer leads quickly to the formation of PICs around this preformed template.[8,10] Non-equilibrium structures of different shapes resulting from the rearrangement of colloidal structures are also observed on a longer timescale.[10] The conformational changes occurring on preformed thermoresponsive

PICs nanostructures upon heating or cooling and the reversibility of these modifications are less studied. The few examples [5-10] described in the literature do not enable the key parameters controlling such behavior to be determined. Macromolecular characteristics such as the polymer chain length and dispersity, block copolymer composition (i.e. the ratio of hydrophilic to hydrophobic parts), residual homopolymer content or structure (branching) are fundamental. To obtain further insight into the influence of these parameters, the association of poly(acrylic acid) (PAA) and a cationic thermoresponsive poly(3-acrylamidopropyl trimethylammonium chloride-*b*-*N*-isopropylacrylamide) (PAPTAC-*b*-PNIPAM, **scheme 1**) with different composition and molar masses is studied here. For each investigated PAPTAC-*b*-PNIPAM/PAA system, the ratio between the cationic and anionic segments was varied to follow the formation of the complexes and discern the mechanism of assemblies' formation. The effect of temperature on such PIC micelles was then monitored with a variety of techniques including light scattering, zeta potential, nuclear magnetic resonance spectroscopy (NMR) and thermal analysis.

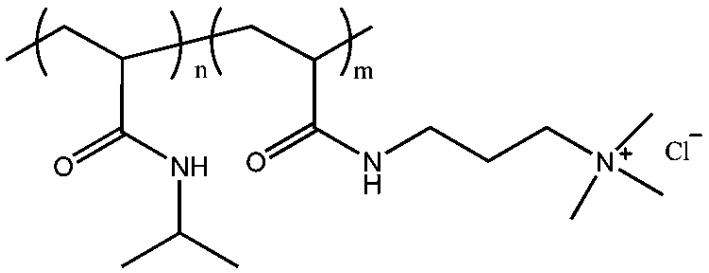

Scheme 1. Chemical structure of the studied PAPTAC-b-PNIPAM diblock copolymers.

2. Materials and Methods

2.1. Materials.

(3-acrylamidopropyl)trimethylammonium chloride solution (APTAC, 75 % (w/w) in water), *N*-isopropylacrylamide (NIPAM, 97 wt.%) and poly(diallyldimethylammonium chloride) (PDADMAC, 20 % (w/w) in water, M_w 200000-350000) were supplied by Sigma-Aldrich and used as received. 2,2'-

Azobis(2-methylpropionamidine)dihydrochloride (V-50, 98%), ammonium persulfate (APS, 98+%), and L(+)-ascorbic acid (AsAc, 99%) were obtained from Acros Organics. *O*-Ehyl-*S*-(1-methoxycarbonyl) ethyldithiocarbonate (XA) was synthesized according to literature.[11] Ethanol and distilled water were used as solvent for polymer syntheses. Water of MilliQ quality (Millipore, Bedford, MA, USA) was used in capillary electrophoresis experiments, as well as fused-silica capillaries with a poly(ethylene oxide) coating (named "WAX", 50 μm i.d., 360 μm o.d., from Agilent). Phosphoric acid (≥99.0 %) was purchased from Fusions (Homebush, Australia). Hexaminecobalt (III) chloride (≥99.5 %), ammonium nitrate (≥98%), acetonitrile (≥99.93%), NaOH (≥98%) and absolute ethanol were supplied by Sigma-Aldrich Chemical Company. PAA_{2k} and PAA_{10k} were synthesized as previously described.[32]

2.2. Polymer synthesis.

A typical procedure for the synthesis of the $PAPTAC_{7.5k}$ first block is as follows: APTAC (10.6 g, 51.4 mmol), XA (0.24 g, 1.15 mmol), V-50 (0.06 g, 0.19 mmol), ethanol (1.81 g) and distilled water (7.39 g) were placed in a 50 ml two-neck round-bottom flask. The solution was degassed by bubbling argon for 30 min before heating at 60 °C for 3h. Conversion was monitored using quantitative ^{1}H NMR by taking aliquots until it reached 100%. The mixture was concentrated under reduced pressure to remove ethanol and then the polymer concentration in the solution was determined by gravimetry (50.7%) to use this PAPTAC-XA solution as macro-RAFT agent for the synthesis of the diblock copolymer. ^{1}H NMR 300 MHz (D_2O) δ : 1.35-1.79 (m, 2H, -CH_2-CH- backbone), 1.84-2.24 (m, 3H, -CH_2-CH- backbone, CONH-CH_2-CH_2-CH_2-N(CH_3)$_3$), 2.98-3.44 (m, 13H, CONH-CH_2-CH_2-CH_2-N(CH_3)$_3$)

A typical procedure for the synthesis of the $PAPTAC_{7.5k}$-$PNIPAM_{12.5k}$ block copolymer is as follows. The PAPTAC-XA solution (11.8 g, 0.78 mmol of XA), NIPAM (9.77 g, 86.0 mmol), APS (0.20 g, 0.86 mmol) and distilled water (15.8 g) were placed in a 100 ml round-bottom flask. The solution was degassed for 30 min by argon bubbling. AsAc (0.15 g, 0.86 mmol) was separately dissolved in 2 g of water and degassed for 30 min in the same way. Then AsAc was added to the mixture to initiate the reaction that was let for 24 h until completion. The solvent was evaporated under reduced pressure and the residue was dissolved in ethanol before precipitating in diethyl ether to give a white powder determined to be the

$PAPTAC_{7.5k}$-***b***-$PNIPAM_{12.5k}$ block copolymer. 10 ml of a 10g/L of block copolymer solution were dialyzed three times against 800 mL of water. Pur-a-LyzerTM Mega dialysis kit MWCO 1000 were used for $PAPTAC_{2k}$-$PNIPAM_{8k}$ and $PAPTAC_{1k}$-$PNIPAM_{9k}$ and 3500 for $PAPTAC_{5k}$-$PNIPAM_{5k}$. The molar ratio of APTAC to NIPAM were determined by ^1H NMR and was in very good agreement with the expected one: APTAC/NIPAM=0.34 (0.33 in theory) ^1H NMR 300 MHz (D_2O) δ : 0.9-1.2 (s, 6H, CONH-CH-$(CH_3)_2$), 1.21-1.75 (m, 2H, -CH_2-CH-backbone), 1.8-2.22 (m, 3H, -CH_2-CH- backbone, CONH-CH_2-CH_2-CH_2-$N(CH_3)_3$), 2.94-3.38 (m, 13H, CONH-CH_2-CH_2-CH_2-$N(CH_3)_3$), 3.68-3.94 (s, 1H, CONH-CH-$(CH_3)_2$).

2.3. Methods.

NMR spectroscopy. ^1H NMR was recorded in D_2O on a Bruker Avance 300 MHz. 3(trimethylsilyl)-propionic acid-d_4 was used as chemical shift internal reference (0 ppm) and as internal standard (relaxation delay equal to 10 s). All the integrals were then calibrated with respect to its signal. The peaks of interest were analyzed for changes in their integral.

Capillary electrophoresis (CE). Capillary Electrophoresis in the Critical Conditions was performed with the technique free solution Capillary Electrophoresis (also known as Capillary Zone Electrophoresis) on an instrument and conditions described in a previous paper.[12] Separations were performed on an Agilent 7100 (Agilent Technologies, Waldbronn, Germany) with a Diode Array Detector (DAD) monitoring at 200 nm with a 10 nm bandwidth. All separations where performed at 30 kV and 25 ºC with a 34.5 cm 'WAX' capillary (effective length 26.0 cm). Samples were injected hydrodynamically with 30 mbar of pressure for 5 s. A 10 mM phosphate buffer at pH 2, used as the background electrolyte (BGE), which was sonicated for 5 min and filtered on 0.2 µm before use. Preconditioning involved a 20 min flush with 10 mM H_3PO_4 followed by a 5 min flush with ethanol and a 10 min flush with the BGE. Between each CE experiments, the capillary was flushed 20 min with 10 mM H_3PO_4 followed by a 5 min with ethanol and 5 min with the BGE After the last CE experiment, the capillary was flushed for 20 min with 10 mM H_3PO_4 then 30 min with ethanol, then 20 min with water and then 5 min with air. Block copolymers were injected at a concentration of 5 g L^{-1}. All samples were dissolved in water containing 1 mM

hexamminecobalt(III) chloride, which was used as an internal standard. Data was plotted and integrated using OriginPro 8.5. The peak areas were corrected by dividing them with the migration time at the relevant apex. The remaining PAPTAC was quantified by a linear calibration of peak area against concentration, using 10 points with 5 concentrations ranging from 0.625 to 5.000 g L^{-1}, R^2 were 0.98 or greater (see **Figure S3c**). For pressure-assisted capillary electrophoresis the same conditions were used except for the addition of 50 mbar of internal pressure throughout the separation.

Size-exclusion chromatography (SEC). SEC of PAPTAC homopolymers was carried out on a Agilent 1100 HPLC system including a vacuum degasser and an isocratic pump monitored by an eclipse 2 system (Wyatt technology), a guard column Shodex SB806-M and 2 Shodex OHpak columns in series (one SB-806M HQ (8 mm*300 mm, 13 µm)+ Shodex OH-pak SB802.5 HQ (8 mm*300 mm, 6 µm)) coated with poly(diallyldimethylammonium chloride) (PDADMAC) coupled with a refractometer (OptilabRex, Wyatt technology), a UV detector (Agilent) set at 290 nm and a multi-angle laser light scattering detector (Dawn Heleos II + QELS, 18 angles, Wyatt technology). The eluent used was 1 M NH_4NO_3 aqueous solution/acetonitrile (80/20, w/w) at pH=2 containing 100 ppm of PDADMAC (flowrate 1 m·/min^{-1}). Samples were prepared at a polymer concentration of 5 g.L^{-1} and filtered through 0.45 µm PTFE filters before injection. In addition to SEC-RI-MALS characterization, average molar masses of PAPTAC were also determined by SEC-RI based on PEO calibration curve (PEO standards with M_p=106, 420, 600, 1500, 3120, 6240, 12000, 23000, 40000, 100000 and 300000 g/mol).

Differential Scanning Calorimetry (DSC). The thermal properties of the polymer (in solution and in bulk) were determined by Differential Scanning Calorimetry (DSC) using a Mettler Toledo DSC 1 STARe System Thermal Analysis calorimeter equipped with a Gas Controller GC200. Solution samples at a concentration equal to 0.5 wt.% were sealed in impermeable crucibles of 120 µL. Transition temperatures were taken at the top of the peak on the thermogram on heating and extrapolated the values obtained at different heating rates to 0 °C/min. The variation of enthalpy was measured as the temperature increased at a rate of 1 °C/min.

Dynamic Light Scattering (DLS). DLS was carried out on a Malvern Zetasizer NanoZS equipped with a He-Ne laser (λ=633 nm) in plastic cuvette on filtered solutions. The correlation function was then analyzed via the general-purpose non-negative least squares (NNLS) method to obtain the intensity-weighted distribution of diffusion coefficients (D) of the solutes. This distribution can be converted, using Mie theory, to a number-weighted distribution describing the relative proportion of multiple components in the sample based on their number rather than based on their scattering. The average apparent hydrodynamic radius, noted as R_h was determined using the Stokes-Einstein equation from number-weighted distribution. The typical accuracy for these measurements was 10-15%. It has to be mentioned that the determination of R_h assumed non interacting particles modeled with a homogeneous spherical hard sphere models.

Small-Angle X-ray Scattering (SAXS). SAXS was performed at the high brilliance beamline ID02 of the European Synchrotron Radiation Facility (ESRF) in Grenoble, France.[13] The 2D SAXS patterns were collected using a Rayonix MX-170HS ccd detector. The measured SAXS profiles were normalized to an absolute scale using the standard procedure reported elsewhere.[14] A combination of two sample-to-detector distances (10 and 1 m) was employed, covering a total q-range from 0.01 to 6 nm^{-1}. q is the scattering wave vector defined as $q = (4\pi/\lambda) \sin \vartheta/2$, λ being the wavelength ($\lambda \sim 1$ Å) and ϑ the scattering angle. The solutions were loaded in a flow through capillary of 2 mm diameter to ensure an accurate subtraction of the background (water) and to minimize beam damage of the samples.

3. Results and discussion

3.1. Polymer synthesis and characterization.

a. Polymer synthesis and purification. A limited number of articles describe the synthesis of PAPTAC-*b*-PNIPAM diblock copolymers and the study of their physicochemical properties, with no focus on their interaction with oppositely charged polymers.[15-18] Although ATRP of 3-acrylamidopropyltrimethylammonium chloride (APTAC) was reported in water-ethanol mixtures,[19] the synthesis of PNIPAM-PAPTAC diblock copolymers by ATRP was only performed in water-DMF (50/50 v/v) at 20 °C.[15-16] In the latter conditions, Patrizi et al. first polymerized APTAC using the CuCl/Me_6TREN catalyst before adding *N*-isopropylacrylamide (NIPAM) according to a "one-pot" protocol.[15] Nyström and coworkers [16-18] slightly modified these conditions by polymerizing NIPAM first with the CuCl/$CuCl_2$/Me_6TREN catalyst before chain extension with APTAC polymerization. A more eco-friendly, metal-free approach is reported here by performing the synthesis of PAPTAC-*b*-PNIPAM diblock copolymers in water at room temperature by means of reversible addition-fragmentation chain transfer (RAFT) polymerization.[20-21] RAFT polymerization was considered here because of its ease of implementation in aqueous media at room temperature with no need for a metal catalyst or hazardous solvent like DMF, and its ability to directly polymerize charged monomers.[22] Contrasting with the rich literature on aqueous RAFT polymerization of charged monomers,[22] only our group reported the RAFT polymerization of the APTAC monomer using a xanthate transfer agent, namely *O*-ethyl-*S*-(1-methoxycarbonyl) ethyl dithiocarbonate (XA).[23-25] In the present study the XA RAFT agent was selected for its ability to control the polymerization of both NIPAM[23,26] and APTAC monomers.

The polymerization of APTAC was initiated by azobis(2-methyl-propionamidine)dihydrochloride (V-50) in the presence of XA at 60 °C in an ethanol-water mixture (1:4 wt. ratio). Polymerization was performed for 3 h until complete monomer conversion, as determined by ^{1}H NMR. Different number-average molar

masses M_n equal to 1000, 2000, 5000 and 7500 g/mol were targeted to assess the control of the polymerization. As shown in **Table 1**, all polymerizations of APTAC were well controlled according to M_n determined by SEC. Dispersities ($Đ$) s of 1.2-1.7 were obtained, due to the relatively slow exchange of the *O*-ethyl xanthate group between dormant and active chains in RAFT polymerization of acrylamides.[27]

Block copolymerization of NIPAM from the PAPTAC-XA precursor was carried out in water at 25 °C, i.e., below the LCST of PNIPAM, using the ammonium persulfate/ascorbic acid redox initiation system. After 24 h of reaction, NIPAM had fully reacted as evidenced by ^{1}H NMR. Block copolymers with different compositions or M_n were obtained. While PAPTAC and PNIPAM homopolymers can be independently characterized by SEC in appropriate conditions (Figure S1 in ESI for the SEC of PAPTAC), the block copolymer did not elute out of the SEC column under any of the eluent-column combinations tested.[25] This is in accordance with the conclusions of Patrizi et al. who tried to characterize similar copolymers by SEC.[15] Due to adsorption onto the stationary phase,[12] aqueous SEC of PNIPAM is usually set aside in favor of DMF/LiBr[21] or methanol eluents.[28] However, SEC analysis of PAPTAC usually requires water/organic solvent mixtures with relatively high salt concentration.[25] Therefore, the determination of molar masses by SEC was impossible for these block copolymers. Alternative chromatographic methods such as liquid chromatography in the critical conditions were not attempted due to the limitations reviewed by D. Berek [29] as well as its limited application to hydrophilic copolymers.

Table 1. Main characteristics of PAPTAC-*b*-PNIPAM samples.

		PAPTAC homopolymer			PAPTAC-*b*-PNIPAM block copolymer			
	Sample	$M_{n,th}$ (g·mol^{-1})	$M_{n,MALS}$[a] (g·mol^{-1}) ($Đ$)	$M_{n,PEO}$[b] (g·mol^{-1}) ($Đ$)	DPn_{APTAC} /$DPn_{NIPAM\ th}$	DP_{nAPTAC} /DP_{nNIPAM} [c]	T_c (°C)[d]	ΔH (J·g^{-1})[e]
1	**PNIPAM$_{10k}$**	/	/	/	0/89	0/89	31.2	35 (35)
2	**PAPTAC$_{1k}$-PNIPAM$_{9k}$**	1000	1760 (1.31)	1450 (1.19)	5/80	5/104	33.4	26 (28)
3	**PAPTAC$_{2k}$-PNIPAM$_{8k}$**	2000	2770 (1.37)	2000 (1.41)	10/72	10/98	33.3	16 (20)
4	**PAPTAC$_{5k}$-PNIPAM$_{5k}$**	5000	5400 (1.54)	4600 (1.72)	24/44	24/49	33.1	12 (24)

5	**$PAPTAC_{7.5k}$-$PNIPAM_{12.5k}$**	7500	8300 (1.51)	7200 (1.61)	36/110	36/115	32.3	20 (28)

[a] determined by SEC-RI-MALS, [b] determined by SEC-RI in H_2O with PEO standards, [c] from NMR results, [d] measured by DSC at different heating rates at a concentration equal to 0.5 wt.% and extrapolated to 0 °C/min for the onset value, [e] enthalpy variation per gram of polymer (per gram of PNIPAM) obtained from DSC measurements with a temperature increase rate of 1 °C/min.

Capillary electrophoresis in the critical conditions (CE-CC) is being developed to characterize complex polyelectrolytes[30]. It has allowed the successful quantification of homopolymers in cationic statistical copolymers[31] and in block copolymers[32] including PAPTAC-*b*-PNIPAM.[12] Pressure-assisted CE-CC separated effectively PAPTAC homopolymer, PNIPAM homopolymer and their diblock copolymer. These polymers are characterized by their distributions of electrophoretic mobilities (Figure 1 and Figure S2-3 in ESI): the electrophoretic mobilities of the block copolymers are lower than the one of PAPTAC homopolymer but higher than the one of PNIPAM homopolymer. The formation of diblock copolymers is thus proven and at the same time 1 to 3 % (w/w) of PNIPAM homopolymer and 2 to 19 % (w/w) of PAPTAC homopolymers were detected (see **Table S1**) as well as short PAPTAC oligomers. This relatively high fraction of dead PAPTAC was unexpected because of the mild initiation conditions used to minimize the generation of dead chains due to classical termination. In addition, the possibility of a slow reactivation of PAPTAC-XA during NIPAM polymerization, leaving a fraction of PAPTAC-XA homopolymer in the final diblock copolymer, was ruled out because it has been established in our earlier works that XA reacts faster than NIPAM during RAFT polymerization. [23,26] Hence, we believe that the moderate reactivity of XA is not responsible for the presence of PAPTAC homopolymer in the diblock copolymer. This result might be related to the presence of impurities (e.g. amines) in the commercial monomer solution, which could chemically degrade a fraction of the xanthate terminal group during polymerization. This is consistent with an increased proportion of dead PAPTAC with increasing ratio of APTAC to XA when synthesizing the first block.

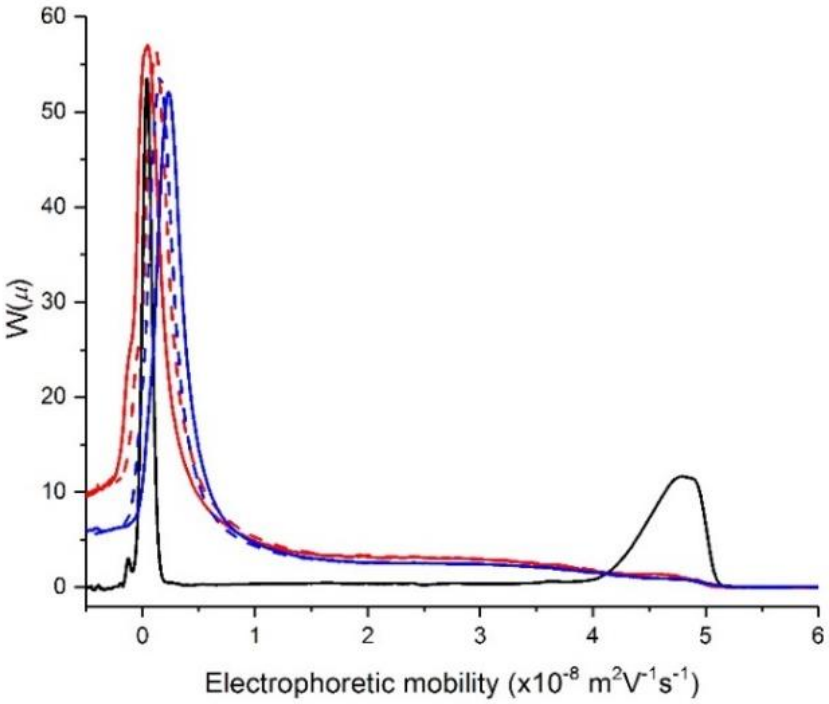

Figure 1. Distributions of electrophoretic mobilities ($W(\mu)$) obtained by pressure-assisted capillary electrophoresis in the critical conditions of a mixture of $PAPTAC_{5k}$ and $PNIPAM_{5k}$ homopolymers (black) as well as of block copolymers $PAPTAC_{2k}$-$PNIPAM_{8k}$ before (red) and after dialysis (blue). Dashed lines indicate repeat separations.

Dialysis was performed in water in order to remove APTAC oligomers. For all polymers a decrease in APTAC monomer units content was measured by NMR (**Table 1**). CE also confirmed the effectiveness of such purification showing that dialysis particularly remove the shortest oligomer chains (**Figure S3a-b**). The amount of remaining PNIPAM homopolymer was not changed by dialysis for most block copolymers (**Table S1** in ESI) indicating a relatively large hydrodynamic volume for the remaining PNIPAM homopolymer. Residual PAPTAC homopolymers slightly decreased to less than 4 and 2% (w/w) for $PAPTAC_{1k}$-$PNIPAM_{9k}$ and $PAPTAC_{2k}$-$PNIPAM_{8k}$, respectively. In the case of more symmetrical $PAPTAC_{5k}$-$PNIPAM_{5k}$ there was 18 % (w/w) of residual PAPTAC due to the difficulty of selectively removing longer PAPTAC dead chains by dialysis. In addition, the composition and

heterogeneity of the diblock copolymers were assessed before and after dialysis through their distributions of electrophoretic mobilities. The weight-average electrophoretic mobility (μ_w) is related to the average composition of the diblock copolymer and the dispersity of the electrophoretic mobility distribution is associated with the heterogeneity of the composition. The μ_w of $PAPTAC_{1k}$-$PNIPAM_{9k}$ and $PAPTAC_{2k}$-$PNIPAM_{8k}$ are similar but $PAPTAC_{1k}$-$PNIPAM_{9k}$ has a higher μ_w which is indicative of a higher fraction of charged units and that the chemical composition of the block copolymers is indeed different (**Table S2** in ESI). After dialysis the μ_w was higher or the same for each diblock copolymer which suggests a slight change in the composition of the block copolymers to a slightly higher PAPTAC fraction. Since NMR analysis showed a decrease in APTC monomer unit, it is likely that the oligomers removed by dialysis were mostly PNIPAM-rich block co-oligomer chains. The dispersity of the electrophoretic mobility distribution of the block copolymers by pressure-assisted CE was between 1.1 and 1.2 for three samples before dialysis showing that all the three samples have similar heterogeneity in terms of chemical composition from the synthesis. After dialysis the dispersity of electrophoretic mobilities increased for $PAPTAC_{5k}$-$PNIPAM_{5k}$. $PAPTAC_{5k}$-$PNIPAM_{5k}$ showed two populations of diblock chains, one which has a higher fraction of APTAC units and another with a higher fraction of NIPAM units both before and after dialysis. After dialysis it appeared that a large portion of the diblock chains with a higher fraction of NIPAM units was removed (**Figure S2** in ESI) and since they are closer to the median composition, this led to a slightly more bimodal distribution hence higher dispersity. However, the μ_w did not change significantly after dialysis suggesting only a change in the heterogeneity of the composition, not of the average composition. The final average composition was therefore evaluated by NMR based on PAPTAC characterization of the first block.

Hence, four different PAPTAC-*b*-PNIPAM thermoresponsive diblock copolymers with different molecular weight and composition (**Table 1**) were synthesized by aqueous RAFT polymerization and fully characterized before the exploration of their physicochemical properties.

b. Behavior of PAPTAC-b-PNIPAM block polymers alone in solution. The behaviour of these copolymers in aqueous solutions was then evaluated through differential scanning calorimetry (DSC), turbidimetry and scattering experiments. Upon heating, all copolymers exhibited a transition temperature T_c, called cloud point temperature, around 33 °C (See **Table 1**). The slight increase in T_c compared to PNIPAM homopolymer (whose T_c is equal to 31.2 °C) was related to the introduction of the hydrophilic PAPTAC block. Below T_c, copolymers present a double hydrophilic character and were thus present in the solution as single polymer chains with a hydrodynamic radius (R_h) below 5 nm as measured by dynamic light scattering (DLS). This value is in good accordance with the value of the radius of gyration (R_g about 5 nm) determined by small-angle X-ray scattering (SAXS) in the case of $PAPTAC_{1k}$-*b*-$PNIPAM_{9k}$ using the form factor of Gaussian polymer chains as a model to fit the data (see I.3 Section and **Figure S4** in ESI). Above the T_c, the PNIPAM block dehydrates. The copolymers become amphiphilic and tend to form large nano-objects with an outer PAPTAC shell as evidenced by DLS and a positive zeta potential. Average R_h values of 78 nm (for $PAPTAC_{1k}$-$PNIPAM_{9k}$) and 150 nm (for $PAPTAC_{2k}$-$PNIPAM_{8k}$ and $PAPTAC_{5k}$-$PNIPAM_{5k}$) were measured by DLS. In addition, SAXS measurements on $PAPTAC_{1k}$-$PNIPAM_{9k}$ allowed the estimation of an average radius of the assembled objects around 98 nm, by modelling the scattering data with the form factor of spherical objects (see I.3 Section and **Figure S4** in ESI). This large size is compatible with the formation of aggregates of nano-objects also named large compound micelles in the literature.[26]

3.2. Formation of polyion complex aggregates and their characterization at room temperature.

The solution behavior of PAPTAC-*b*-PNIPAM copolymers was then studied in the presence of PAA with two different chain lengths: PAA_{2k} and PAA_{10k}. For this, a stock solution of PAPTAC-*b*-PNIPAM at pH 7 was diluted with the adequate amount of water and then different volumes of PAA stock solution at pH 7 (adjusted with NaOH) were added at room temperature. The samples had a final block copolymer concentration of 0.5 % (w/w) and varied *R*, defined as the molar ratio between AA and APTAC monomer units. **Figure 2** shows the typical trend of the scattered light intensity (A) and zeta potential (B) for the

objects formed from the association of $PAPTAC_{1k}$-$PNIPAM_{9k}$ with PAA_{2k} measured by DLS below (25 °C) and above T_c (45 °C) as a function of the molar ratio, *R* (additional data for $PAPTAC_{5k}$-$PNIPAM_{5k}$ can be found in supplementary information, **Figures S5**).

.

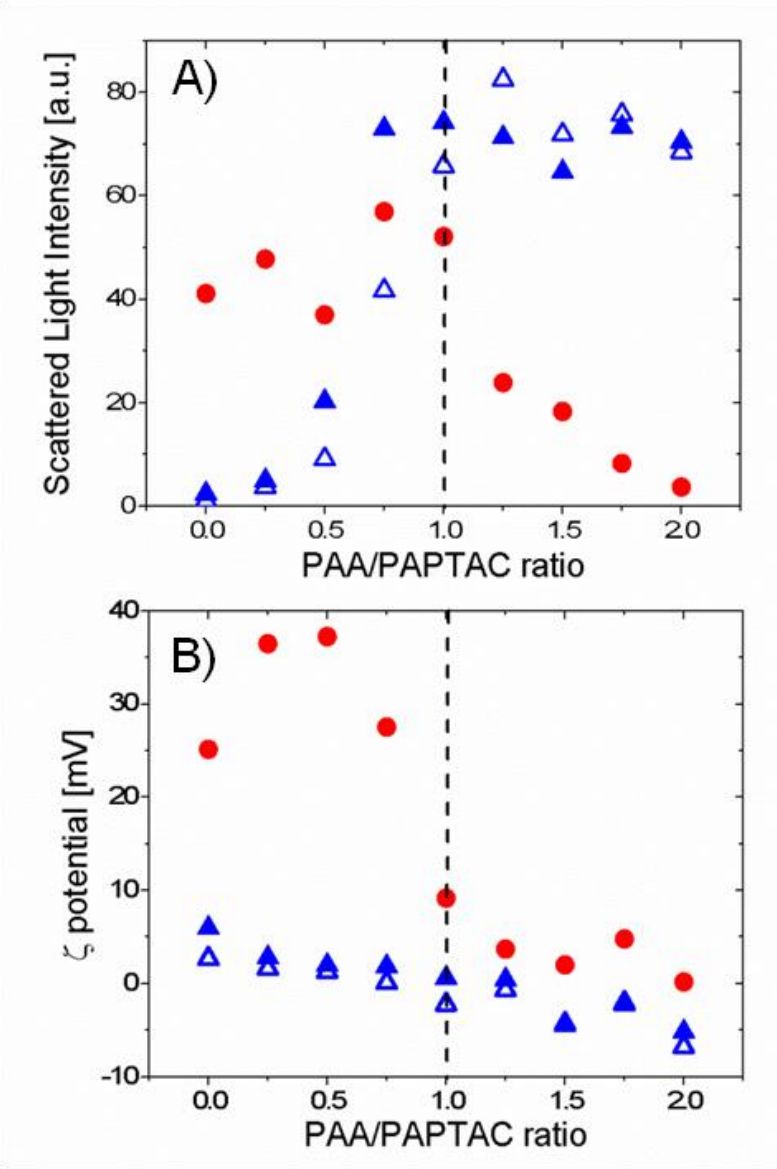

Figure 2. A) Scattered light intensity and B) ζ potential of 0.5 wt.% $PAPTAC_{1k}$-$PNIPAM_{9k}$ aqueous solution at different PAA_{2k}/PAPTAC molar unit ratios at 25 °C (open blue triangles), 45 °C (red circles) and back to 25 °C (filled blue triangles).

At 25 °C, the scattered light intensity increased with increasing molar ratio to reach a plateau when *R* is higher than 1. This trend reflects the formation of PIC aggregates resulting from the electrostatic interaction between the positively charged APTAC units and the negatively charged acrylate units. Moreover, even if the influence of a small amount of homopolymer (3.8 wt.%) in the block polymer solution could not be completely excluded, we assume that its effect is not critical on the observed aggregation behavior effect. Indeed, aggregation behavior was found to be identical before and after partial removal of homopolymer from copolymer solution. This complex formation was confirmed by ^{1}H NMR spectra recorded at 25 °C: when PIC objects were formed in solution, the integral of the peaks corresponding to ester groups of PAPTAC (mixing ratio around 1) was about 80% of the initial integral and it remained roughly constant for higher molar ratios (**Figure 3B** and **Figure S8** in ESI). This can be attributed to the loss of mobility of the ammonium groups when they associate to the AA groups inside the aggregate. The peaks did not completely disappear, probably due to the high water content inside the aggregates.[7]

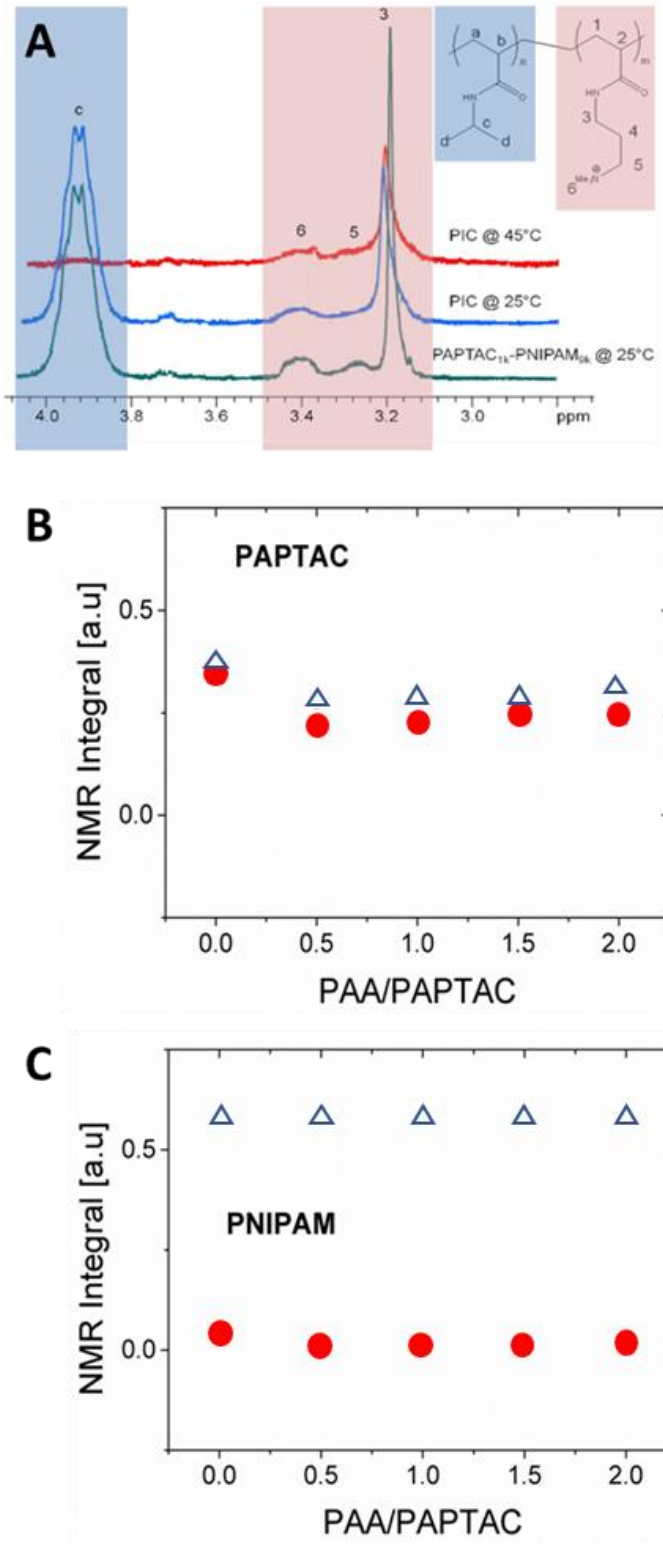

Figure 3. A. ^{1}H NMR spectra (D_2O, 300 MHz) of t $PAPTAC_{1k}$-*b*-$PNIPAM_{9k}$ at 0.5 % (w/w) alone at 25 °C (green curve), with PAA_{2k} R = 1 at 25 °C (blue curve) and at 45 °C (red curve). B and C. Trend of the integrals of the signals relative to B) PAPTAC (between 3.1 and 3.5 ppm) and C) PNIPAM (3.91 ppm) at 25 °C (open blue triangles) and 45 °C (filled red circles) as a function of the PAA/PAPTAC molar ratio.

Besides, the electrostatic driving force was confirmed by micelles dissociation following salt addition with a critical salt concentration of 125-250 mmol.L^{-1}, typical of this kind of assemblies (**Figures S9** and **S10** in ESI). [5,7] The trend of the ζ potential of the objects at 25 °C in **Figure 2B** completes the picture: as expected, the zeta potential decreased while increasing the mixing ratio and it became slightly negative with an excess of PAA. Nano objects with a characteristic R_h around 30 nm were evidenced by DLS. This size is slightly smaller than the one observed in literature for thermoresponsive PICs.[33] SAXS and static light scattering (SLS) measurements were performed for ratios equal to R= 0, 0.5 and 1 to gain a detailed picture of the formation and the morphology of PICs at 25°C (**Figure 4**).

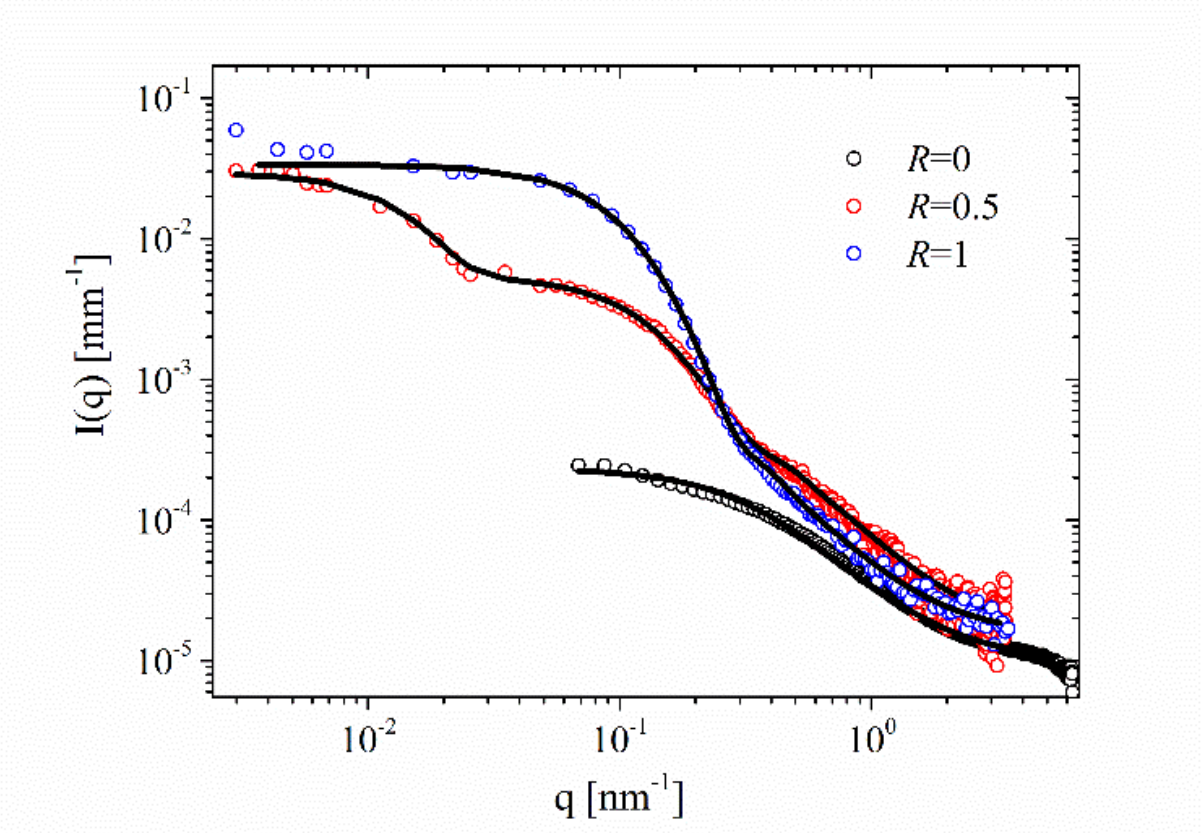

Figure 4. Scattering curves of PAPTAC$_{1k}$-PNIPAM$_{9k}$ (1 % (w/w)) with PAA$_{2k}$ in aqueous solution at 25°C for different ratios R = 0, 0.5 and 1. Additional data and fit for 45°C are presented in Figure S11.

As previously mentioned, $PAPTAC_{1k}$-$PNIPAM_{9k}$ are dispersed in the solution like free gaussian polymer chains with a radius of gyration, R_g, of approximately 5 nm. After mixing the copolymer with PAA_{2k}, a strong increase of the scattering signal at low-q is measured for R=0.5. The scattering intensity increased with increasing molar ratios of PAA_{2k} until R=1. From the Zimm analysis of the SLS data, a R_g of approximately 55 nm was estimated when R=1 and the data could be described by assuming a cylindrical morphology for the aggregates (radius of the core R_c=11.8 nm and length of the cylinder L=47 nm) with a PNIPAM shell and a PAA-PAPTAC core (see section II.4 in ESI). Furthermore, the behavior of the high-q region of the scattering curves ($I(q) \propto q^{-1.5}$) was described, with an additional contribution to the model which takes into account the inter-chain interactions among the two polymer components.[14]

The scattering curve relative to R=0.5 clearly shows the presence of populations of different sizes: two well defined Guinier regions can be recognized as corresponding to nano-objects with an average R_g of 13 nm and R_g=151 nm, respectively. Additionally, at high-q, the contribution to the scattering signal due to polymer inter-chain interactions is higher with respect to the curve at R=1, suggesting the presence of free polymer chains in solution. The data were well described with the coexistence of free polymer chains of R_g=5 nm, cylindrical micelles corresponding to PICs obtained at R=1 (R_c = 10.2 nm, L = 40 nm) and large spherical aggregates (R_s= 120 nm). It is worth noting from the ratio between the intensity levels of the Guinier regions of the two populations (Figure 4, R=0.5), that the concentration of these big aggregates is negligible (i.e. about 3-4 million times lower) compared to that of the small cylinders.

Hence, at 25°C, as evidenced by NMR and scattering measurements, the interaction of PAPTAC-*b*-PNIPAM copolymers with PAA led to the formation of PICs aggregates starting from a molar ratio R= 0.5.

3.3. Effect of temperature on the structure of PICs and reversibility of the transition. Starting from PIC assemblies at 25 °C, temperature was then increased to 45 °C, above the T_c of the PNIPAM block. At 45°C, PNIPAM is partially dehydrated and the block copolymer presents an amphiphilic character. Therefore, in solution and in the presence of PAA, two different driving forces might compete in the aggregation process: electrostatic interactions between PAPTAC and PAA and hydrophobic forces between the insoluble PNIPAM blocks. Different behaviors were observed when increasing the temperature above T_c depending on (a) the molar ratio of AA to APTAC and (b) the structural parameters (molecular weight, composition, purity, branching) of the polymers.

a. Effect of molar ratio. The observed transformation at different molar ratios *R* will be discussed for the $PAPTAC_{1k}$-$PNIPAM_{9k}$ complexed with PAA_{2k}. For molar ratios lower than or equal to 1, when heating above T_c an increase in both solution turbidity and scattered light intensity were observed suggesting the formation of large objects (**Figure 2A**). Simultaneously, the zeta potential of the objects is high and positive for low *R* ratios indicating the presence of nano-objects where the PAPTAC block is more exposed to the solvent. For *R* values equal to or higher than 1, the zeta potential has a low absolute value (**Figure 2B**). In addition, a dramatic decrease in the peaks relative to the isopropyl protons of the PNIPAM units at 3.91 ppm was observed in ^{1}H NMR (**Figure 3A** and **3C**). This phenomenon might be ascribed to partial dehydration of PNIPAM groups. The signal intensity of the PAPTAC methyl protons (between 3.1 and 3.5 ppm) also slightly decreased when the temperature increased (**Figure 3B**) in agreement with the formation of larger objects. In addition, when the solutions were cooled back to 25 °C, the scattered intensity returned quickly, in few seconds, to its initial value (**Figure 2A**). Hence the transformation of $PAPTAC_{1k}$-$PNIPAM_{9k}$ complexed with PAA_{2k} is fast and fully reversible.

To explain these results, two scenarios are evocated. Firstly, for molar ratios up to 1, PICs might coexist at 25 °C with free uncomplexed $PAPTAC_{1k}$-$PNIPAM_{9k}$ copolymers. This would result at 45 °C in the presence of different families of aggregates. The first family would originate from PICs: electrostatic interactions enable to lock the core of PICs structure obtained at 25 °C, and above T_c PICs present an

external dehydrated PNIPAM shell. This formation is illustrated in **Scheme 2**. Hydrophobic 'interactions' between the dehydrated PNIPAM shells of PICs would induce the formation of large nano-objects similar to the phenomenon observed previously with a poly(*n*-butyl acrylate)-*b*-poly(*N*-isopropylacrylamide), PnBA-*b*-PNIPAM amphiphilic block copolymer.[26] As observed here, PnBA-*b*-PNIPAM copolymers undergo a fast and reversible process from micelle to aggregates of micelles when changing temperature around T_c. These aggregates of PICs are expected to have a zeta potential close to zero.

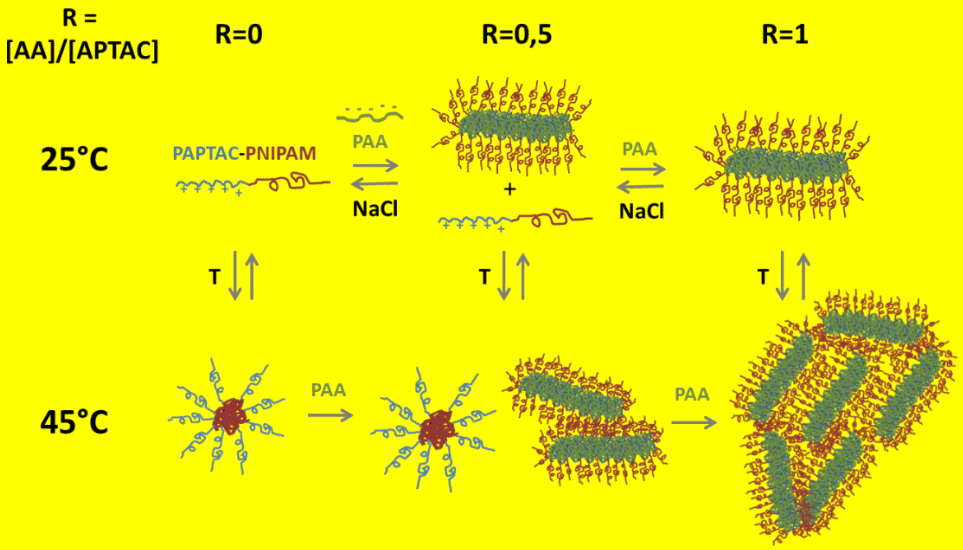

Scheme 2. Main transitions occurring through changes in temperature or ionic strength.

The positive zeta potential value measured for *R* ratios lower than one (**Figure 2B**) at 45°C might be then ascribed to the presence in solution of the second family of aggregates which originates from partially or uncomplexed PAPTAC-PNIPAM block copolymers. These block copolymers switch from a soluble to amphiphilic character at 45°C and their aggregation might result in the formation of large aggregates with a PNIPAM dehydrated core and a PAPTAC corona, as discussed before. The presence of such aggregates results in a positive zeta potential.[22] Both families of nano-objects (aggregates of PICs and micelles of PAPTAC-*b*-PNIPAM) would explain the positive zeta potential measured and the decrease in zeta potential to near 0 when free block copolymer is no longer present.

Another mechanism might take place when the temperature is increased if electrostatic interactions do not lock the PICs structures. In this case, PNIPAM-PAPTAC micelles with an outer PAPTAC shell would be formed and could be further complexed with surrounding PAA polymers. The observed fast reversible process led us to discard this second mechanism which would require more complex phenomena to occur. Nonetheless, in order to settle the question, we performed SAXS structural investigations. The scattering curves relative to molar ratios *R* equal to 0, 0.5 and 1 at T=45°C are represented in **Figure S11** and all the results are summarized in **Table S3**. In the case of *R*=1 (blue curve in Figure S11), the scattering trend as a function of the scattering vector, *q*, shows the presence of large nano-objects in solution. At high-*q* the signature of their polymeric nature is lost and an extended Porod region with a slope of -4 is present. Using a Guinier-Porod model analysis of the plateau at low-*q*, a R_g of 250 nm was estimated. As for *R*=0.5 (red curve in Figure S11), the scattering curve resembles that of the copolymer alone, but it presents an extra scattering contribution at intermediate *q* values. This cannot be correctly described with only one population of objects. The scattering patterns were best modelled with a mixture of spherical objects of approximately the same size as those found at *R*=0 (R_s= 79 nm) at T=45°C and cylindrical PIC assemblies similar to those found at *R*=0.5 and *R*=1 for T=25°C (R_c=11.8 nm and *L*=47 nm). The structural studies confirmed our first scenario: PICs are still present above T_c due to the strong attractive electrostatic interactions between PAA and PAPTAC blocks. At high temperatures, for *R*= 1 the formation of big aggregates of PICs are induced by the hydrophobic interactions between the dehydrated PNIPAM shells. The lower concentration of PICs and/or the presence of positively charged assemblies (the spherical assemblies with a PNIPAM core corresponding to *R*=0) at *R*=0.5 prevents the aggregation at high temperature.

At mixing molar ratios higher than 1, free PAA polymers are present in addition to PICs or PIC aggregates at 25°C or 45°C, respectively. The aggregates observed at 45°C might result from a bridging effect between former nanoobjects due to the interaction of the excess PAA with dehydrated PICs assemblies. A partial precipitation in solution occurred, explaining the decrease in the measured scattered intensity

and the zeta potential with a low absolute value around 0 mV (**Figure 2**). Once again, the assembly process was fast (within a few seconds) and fully reversible.

b. Effect of macromolecular architecture. Similar PICs formation was found for $PAPTAC_{5k}$-$PNIPAM_{5k}$ with PAA_{2k} and reversible conformational changes were also observed above the cloud point temperature (**Figure S5-S8** in ESI). It is also important to point out that for $PAPTAC_{5k}$-$PNIPAM_{5k}$ the presence of a higher homopolymer content in the initial diblock solution (17.8 wt.%) may have an influence on the morphology of the objects obtained after complexation.

Interestingly, the reversibility of the conformational change observed when changing temperature around Tc was partially lost while increasing the molar mass and branching of the polymers. This was first observed when PICs formation was induced by using a different PAA chain, PAA_{10k}, with $PAPTAC_{1k}$-$PNIPAM_{9k}$ or $PAPTAC_{5k}$-$PNIPAM_{5k}$. Compared to PAA_{2k}, PAA_{10k} is longer and slightly more branched (with degree of branching below 2 %) [34,35] and may exhibit a different solubility. Once heated above T_c, the initial scattered intensity (and R_h) were not always recovered when the temperature was lowered back below T_c especially with high content of PAA (See **Figures S12** in ESI). Moreover, this loss of reversibility was more pronounced in the case of $PAPTAC_{7.5k}$-$PNIPAM_{12.5k}$. Precipitation occurred above T_c and the precipitate did not dissolve at 25 °C even after several weeks. While the solution behavior of the objects was not reversible, the hydrophilic-hydrophobic PNIPAM transition always was. This reversibility was evidenced by differential scanning calorimetry (DSC) analysis, as the enthalpy linked to the PNIPAM hydration was unchanged and equal to 28 J/g independently of the mixing ratio (data not shown). Therefore, for high molecular weights, interactions that occurred between the different PIC micelles and PAA leading to the formation of large aggregates could not be counterbalanced once decreasing the temperature below T_c leading to the formation of large and poorly soluble aggregates. This hypothesis is corroborated by the effect of salt addition at 25 °C to solutions of $PAPTAC_{7.5k}$-$PNIPAM_{12.5k}$ showing extensive precipitation. The precipitate completely dissolved at NaCl concentration of 0.5 $mol.L^{-1}$ was used **(Figure S13** in ESI).

4. Conclusions

An innovative aqueous RAFT polymerization strategy was proposed to synthesize PNIPAM-*b*-PAPTAC cationic thermo-responsive block copolymers. Capillary electrophoresis in the critical conditions was then successfully used to characterize them and assess their final composition. Thermoresponsive polyion complex aggregates were then obtained by addition of polyacrylic acid to diblock copolymers based on cationic poly(3-acrylamidopropyltrimethylammonium chloride) and thermoresponsive poly(N-isopropylacrylamide). Above the cloud point temperature, the formed nano-aggregates underwent significant structural changes. Whereas the few examples of thermoresponsive PICS described in the literature do not enable to determine the key parameters controlling such behavior[5-10], we demonstrate here that the aggregation behavior depends on the initial composition of the PICs mixture and on the structural parameters of the different polymers. Moreover, the reversibility of this phenomenon was impeded when block copolymers of high molar mass were considered. This could be utilized in further studies of these block copolymers to lock specific structures obtained from their self-organization for applications such as drug delivery systems.[36]

ACKNOWLEDGMENT. The authors thank B. Amouroux, K.S. Pembe and C. Toppan for their contribution and EU (FEDER-35477 "Nano-objets pour la biotechnologie") for financial support. Michael Sztucki (ID02, ESRF) is acknowledged for his assistance during the beamtime. ESRF is acknowledged for provision of beamtime. AS acknowledges the Australian Commonwealth government for an RTP scholarship.

References

[1] V.A. Kabanov, Basic Properties of Soluble Interpolyelectrolyte Complexes Applied to Bioengineering and Cell Transformations. In Macromolecular Complexes in Chemistry and Biology, Dubin, P.; Bock, J.; Davis, R.; Schulz, D. N.; Thies, C., Eds. Springer Berlin Heidelberg: Berlin, Heidelberg, 1994; pp 151-174.

[2] V. A. Kabanov, Soluble interpolymeric complexes as a new class of synthetic polyelectrolytes, *Pure and Applied Chemistry* **1984,** *56* (3), 343-354. https://doi.org/10.1351/pac198456030343.

[3] A. Harada, K. Kataoka, Chain length recognition: core-shell supramolecular assembly from oppositely charged block copolymers, *Science* **1999**, *283*, 65, https://doi.org/10.1126/science.283.5398.65.

[4] D.V. Pergushov, A.H.E. Muller, F.H. Schacher, Micellar interpolyelectrolyte complexes, *Chem. Soc. Rev*. **2012**, *41*, 6888-6901, https://doi.org/10.1039/C2CS35135H.

[5] I.K. Voets, P.M. Moll, A. Aqil, C. Jerome, C. Detrembleur, P. de Waard, A. de Keizer, M.A. Cohen Stuart, Temperature Responsive Complex Coacervate Core Micelles With a PEO and PNIPAAm Corona, *J. Phys. Chem. B* **2008**, *112*, 10833-10840, https://doi.org/10.1021/jp8014832.

[6] J. Li, W.D. He, N. He, S.C. Han, X.L. Sun, L.Y. Li., B.Y. Zhang, Synthesis of PEG - PNIPAM - PLys hetero - arm star polymer and its variation of thermo - responsibility after the formation of polyelectrolyte complex micelles with PAA, *J. Polym. Sci: Part A: Polym. Chem.* **2009**, *47*, 1450-1462, https://doi.org/10.1002/pola.23254.

[7] S. de Santis, R.D. Ladogana, M. Diociaiuti, G. Masci, Pegylated and Thermosensitive Polyion Complex Micelles by Self-Assembly of Two Oppositely and Permanently Charged Diblock Copolymers, *Macromolecules* **2010**, *43*, 1992-2001, https://doi.org/10.1021/ma9026542.

[8] L. Yuting, B.S. Lokitz, C.L. McCormick, Thermally responsive vesicles and their structural "locking" through polyelectrolyte complex formation, *Angew. Chem. Int. Ed.* **2006**, *45*, 5792-5795, https://doi.org/10.1002/anie.200602168.

[9] C. Dähling, G. Lotze, M. Drechsler, H. Mori, D.V. Pergushov, F.A. Plamper, Temperature-induced structure switch in thermo-responsive micellar interpolyelectrolyte complexes: toward core–shell–corona and worm-like morphologies, *Soft Matter* **2016**, *12*, 5127-5137, https://doi.org/10.1039/C6SM00757K.

[10] C. Dähling, G. Lotze, H. Mori, D.V. Pergushov, F.A. Plamper, Thermoresponsive Segments Retard the Formation of Equilibrium Micellar Interpolyelectrolyte Complexes by Detouring to Various Intermediate Structures, *J. Phys. Chem. B* **2017**, *121*, 6739-6748, https://doi.org/10.1021/acs.jpcb.7b04238.

[11] X. Liu, O. Coutelier, S. Harrisson, T. Tassaing, J.D. Marty and M. Destarac, Enhanced Solubility of Polyvinyl Esters in scCO2 by Means of Vinyl Trifluorobutyrate Monomer, *ACS Macro Lett.*, **2015**, *4*, 89-93, https://doi.org/10.1021/mz500731p.

[12] A.T. Sutton, E. Read, A.R. Maniego, J.J. Thevarajah, J.-D. Marty, M. Destarac, M. Gaborieau, P. Castignolles, Purity of double hydrophilic block copolymers revealed by capillary electrophoresis in the critical conditions, *J. Chromatogr. A* **2014**, *1372*, 187-195, https://doi.org/10.1016/j.chroma.2014.10.105.

[13] T. Narayanan, M. Sztucki, P. Van Vaerenbergh, J. Le´onardon, J. Gorini, L. Claustre, F. Sever, J. Morse and P. Boesecke, A multipurpose instrument for time-resolved ultra-small-angle and coherent X-ray scattering, *J. Appl. Cryst.*, **2018**, 51, 1511-1524, https://doi.org/10.1107/S1600576718012748.

[14] S. Gineste, E. Di Cola, B. Amouroux, U. Till, J.-D. Marty, A.-F. Mingotaud, C. Mingotaud, F. Violleau, D. Berti, G. Parigi, C. Luchinat, S. Balor, M. Sztucki, and B. Lonetti, Mechanistic Insights into Polyion Complex Associations, *Macromolecules*, **2018**, 51(4), 1427-1440, https://doi.org/10.1021/acs.macromol.7b02391.

[15] M.L. Patrizi, M. Diociaiuti, D. Capitani, G. Masci, Synthesis and association properties of thermoresponsive and permanently cationic charged block copolymers, *Polymer* 2009, **50**, 467-474, https://doi.org/10.1016/j.polymer.2008.11.023.

[16] A. Dedinaite E. Thormann, G. Olanya, P.M. Claesson, B. Nyström, A.-L. Kjoniksen, K. Zhu, Friction in aqueous media tuned by temperature-responsive polymer layers, *Soft Matter* **2010**, *6*, 2489-2498, https://doi.org/10.1039/C003320K.

[17] A. Shovsky, S. Knohl, A. Dedinaite, K. Zhu, A.-L. Kjoniksen, B. Nyström, P. Linse, P.M. Claesson, Cationic Poly(N-isopropylacrylamide) Block Copolymer Adsorption Investigated by Dual Polarization Interferometry and Lattice Mean−Field Theory, *Langmuir* **2012**, *28*, 14028-14038, https://doi.org/10.1021/la302154p.

[18] M.T. Calejo, A.M.S. Cardoso, A.-L. Kjoniksen, K. Zhu, C. M. Morais, S. A. Sande, A. L. Cardoso, M.C. Pedroso de Lima, A. Jurado, B. Nyström, Temperature-responsive cationic block copolymers as nanocarriers for gene delivery, *Int. J. Pharmaceutics* **2013**, *448*, 1, 105-114, https://doi.org/10.1016/j.ijpharm.2013.03.028.

[19] P.V. Mendonça, D. Konkolewicz, S.E. Averick, A.C. Serra, A.V. Popov, T. Guliashvili, K. Matyjaszewski, J.F.J. Coelho, Synthesis of cationic poly((3-acrylamidopropyl)trimethylammonium chloride) by SARA ATRP in ecofriendly solvent mixtures, *Polym. Chem.* **2014**, *5*, 5829-5836, https://doi.org/10.1039/C4PY00707G.

[20] W. Bai, L. Zhang, R. Bai, G. Zhang, A Very Useful Redox Initiator for Aqueous RAFT Polymerization of N - Isopropylacrylamide and Acrylamide at Room Temperature, *Macromol. Rapid Commun.* **2008**, 29,7, 562-566, https://doi.org/10.1002/marc.200700823.

[21] A. Guinaudeau, S. Mazières, D.J. Wilson, M. Destarac, Aqueous RAFT/MADIX polymerisation of N-vinyl pyrrolidone at ambient temperature, *Polym. Chem.* **2012**, *3*, 81-84, https://doi.org/10.1039/C1PY00373A.

[22] A.B. Lowe, C.L. McCormick, Reversible Addition–Fragmentation Chain Transfer (RAFT) Radical Polymerization and the Synthesis of Water-Soluble (Co)Polymers under Homogeneous

Conditions in Organic and Aqueous Media, *Prog. Polym. Sci.* **2007**, *32*, 283-351, https://doi.org/10.1016/j.progpolymsci.2006.11.003.

[23] M Beija, E. Palleau, S. Sistach, X. Zhao, L. Ressier, C. Mingotaud, M. Destarac, J.-D. Marty, Control of the catalytic properties and directed assembly on surfaces of MADIX/RAFT polymer-coated gold nanoparticles by tuning polymeric shell charge, *J. Mater. Chem.*, **2010**, *20*, 9433-9442, https://doi.org/10.1039/C0JM01781G.

[24] A. Guinaudeau, O. Coutelier, A. Sandeau, S. Mazières, H.D. Nguyen Thi, V. Le Drogo, D.J. Wilson, M. Destarac, Facile Access to Poly(N-vinylpyrrolidone)-Based Double Hydrophilic Block Copolymers by Aqueous Ambient RAFT/MADIX Polymerization, *Macromolecules*, **2014**, *47*, 41-50, https://doi.org/10.1021/ma4017899.

[25] M. Destarac, I. Blidi, O. Coutelier, A. Guinaudeau, S. Mazières, E. Van Gramberen, J. Wilson, Aqueous RAFT/MADIX Polymerization: Same Monomers, New Polymers?, *ACS Symp. Ser., Vol. 1100, Progress in Controlled Radical Polymerization: Mechanisms and Techniques*, **2012**, 259-275, https://doi.org/10.1021/bk-2012-1100.ch017.

[26] S. Sistach, M. Beija, V. Rahal, A. Brûlet, J.-D. Marty, M. Destarac, C. Mingotaud, Thermoresponsive Amphiphilic Diblock Copolymers Synthesized by MADIX/RAFT: Properties in Aqueous Solutions and Use for the Preparation and Stabilization of Gold Nanoparticles, *Chem. Mater.* **2010**, *22*, 3712-3724, https://doi.org/10.1021/cm100674p.

[27] E. Girard, J.-D. Marty, B. Ameduri, M. Destarac, Direct Synthesis of Vinylidene Fluoride-Based Amphiphilic Diblock Copolymers by RAFT/MADIX Polymerization, *ACS Macro. Lett.* **2012**, *1*, 270-274, https://doi.org/10.1021/mz2001143.

[28] T. Swift, R. Hoskins, R. Telford, R. Plenderleith, D. Pownall, S. Rimmer, Analysis using size exclusion chromatography of poly(N-isopropyl acrylamide) using methanol as an eluent, *J. Chromatogr. A.*, **2017**, 1508, 16-23, https://doi.org/10.1016/j.chroma.2017.05.050.

[29] D. Berek Critical assessment of "critical" liquid chromatography of block copolymers. *J. Sep. Sci.* **2016**, *39* (1), 93-101, https://doi.org/10.1002/jssc.201500956.

[30] J.J. Thevarajah, M. Gaborieau, P. Castignolles, Separation and Characterization of Synthetic Polyelectrolytes and Polysaccharides with Capillary Electrophoresis, *Adv. Chem.*, **2014**, 2014, 798503, https://doi.org/10.1155/2014/798503.

[31] N. Anik, M. Airiau, M.-P. Labeau, C.-T. Vuong, H. Cottet, Characterization of cationic copolymers by capillary electrophoresis using indirect UV detection and contactless conductivity detection, *J. Chromatogr. A* **2012**, *1219*, 188-194, https://doi.org/10.1016/j.chroma.2011.11.014.

[32] M. Jacquin, P. Muller, R. Talingting-Pabalan, H. Cottet, J.-F. Berret, T. Futterer, O. Théodoly, Chemical analysis and aqueous solution properties of charged amphiphilic block copolymers PBA-b-PAA synthesized by MADIX, *J. Colloid Interf. Sci.* **2007**, *316*, 897-911, https://doi.org/10.1016/j.jcis.2007.08.025.

[33] J. Zhang, Y. Zhou, Z. Zhu, Z. Ge and S. Liu, Polyion Complex Micelles Possessing Thermoresponsive Coronas and Their Covalent Core Stabilization via "Click" Chemistry, *Macromolecules,* **2008**, *41*, 1444-1454, https://doi.org/10.1021/ma702199f.

[34] A.R. Maniego, A.T. Sutton, Y. Guillaneuf, C. Lefay, M. Destarac, C. Fellows, P. Castignolles and M Gaborieau, Degree of branching in poly(acrylic acid) prepared by controlled and conventional radical polymerization, *Polym. Chem.*, **2019**, *10*, 2469-2476, https://doi.org/10.1039/C8PY01762J.

[35] A.R. Maniego, A.T. Sutton, M. Gaborieau, P. Castignolles, Assessment of the Branching Quantification in Poly(acrylic acid): Is It as Easy as It Seems?, *Macromolecules* **2017**, *50*, 9032-9041, https://doi.org/10.1021/acs.macromol.7b01411.

[36] M. Beija, R. Salvayre, N. Lauth-de Viguerie and J.-D. Marty, Colloidal systems for drug delivery: from design to therapy, *Trends Biotechnol.,* **2012**, 30, 485-496, https://doi.org/10.1016/j.tibtech.2012.04.008.

Figure captions:

Scheme 1. Chemical structure of the studied PAPTAC-b-PNIPAM diblock copolymers.

Figure 1. Distributions of electrophoretic mobilities ($W(\mu)$) obtained by pressure-assisted capillary electrophoresis in the critical conditions of a mixture of $PAPTAC_{5k}$ and $PNIPAM_{5k}$ homopolymers (black) as well as of block copolymers $PAPTAC_{2k}$-$PNIPAM_{8k}$ before (red) and after dialysis (blue). Dashed lines indicate repeat separations.

Figure 2. A) Scattered light intensity and B) ζ potential of 0.5 wt% $PAPTAC_{1k}$-$PNIPAM_{9k}$ aqueous solution at different PAA_{2k}/PAPTAC molar unit ratios at 25 °C (open blue triangles), 45 °C (red circles) and back to 25 °C (filled blue triangles).

Figure 3. A. ^{1}H NMR spectra (D_2O, 300 MHz) of t $PAPTAC_{1k}$-*b*-$PNIPAM_{9k}$ at 0.5 % (w/w) alone at 25 °C (green curve), with PAA_{2k} R = 1 at 25 °C (blue curve) and at 45 °C (red curve). B and C. Trend of the integrals of the signals relative to B) PAPTAC (between 3.1 and 3.5 ppm) and C) PNIPAM (3.91 ppm) at 25 °C (open blue triangles) and 45 °C (filled red circles) as a function of the PAA/PAPTAC molar ratio.

Figure 4. Scattering curves of $PAPTAC_{1k}$-$PNIPAM_{9k}$ (1 % (w/w)) with PAA_{2k} in aqueous solution at 25°C for different ratios R = 0, 0.5 and 1. Additional data and fit for 45°C are presented in Figure S11.

Scheme 2. Main transitions occurring through changes in temperature or ionic strength.

Table 1. Main characteristics of PAPTAC-*b*-PNIPAM samples.

		PAPTAC homopolymer			PAPTAC-*b*-PNIPAM block copolymer			
	Sample	$M_{n,th}$ (g·mol^{-1})	$M_{n,MALS}$[a] (g·mol^{-1}) (*Đ*)	$M_{n,PEO}$[b] (g·mol^{-1}) (*Đ*)	DPn_{APTAC} /$DPn_{NIPAM\ th}$	DP_{nAPTAC} /DP_{nNIPAM} [c]	T_c (°C)[d]	Δ*H* (J·g^{-1})[e]
1	**PNIPAM$_{10k}$**	/	/	/	0/89	0/89	31.2	35 (35)
2	**PAPTAC$_{1k}$-PNIPAM$_{9k}$**	1000	1760 (1.31)	1450 (1.19)	5/80	5/104	33.4	26 (28)
3	**PAPTAC$_{2k}$-PNIPAM$_{8k}$**	2000	2770 (1.37)	2000 (1.41)	10/72	10/98	33.3	16 (20)
4	**PAPTAC$_{5k}$-PNIPAM$_{5k}$**	5000	5400 (1.54)	4600 (1.72)	24/44	24/49	33.1	12 (24)
5	**PAPTAC$_{7.5k}$-PNIPAM$_{12.5k}$**	7500	8300 (1.51)	7200 (1.61)	36/110	36/115	32.3	20 (28)

[a] determined by SEC-RI-MALS, [b] determined by SEC-RI in H_2O with PEO standards, [c] form NMR results, [d] measured by DSC at different heating rates and extrapolated to 0 °C/min for the onset value, [e] enthalpy variation per gram of polymer (per gram of PNIPAM) obtained from DSC measurements with a temperature increase rate of 1 °C/min.